Numerical Implementation of Source Terms to Evaluate Active Porosity Control using a Transpiration Cooled Thermal Protection System

Caroline Anderson[1], Michael Kinzel[2]
University of Central Florida, Orlando, Florida, 32816 USA
Andrew Brune[3]
NASA Langley Research Center, Hampton Virginia 23681 USA

Transpiration cooling has renewed interest of study as a renewable system of thermal protection for atmospheric entry systems. The presence of coolant within the void space of a porous material changes its effective porosity and theorized to lend the external heatshield as a potential means of porous surface control. Effective porosity is explored in two forms: saturation of void space where exiting coolant creates 'blowing' over the surface, and partial evacuation of the void space where withdrawal of the coolant creates 'suction' on the surface. Thus this study evaluates using transpiration cooling as a as means of active aerodynamic control. The feasibility of the system is evaluated numerically using Reynolds-averaged Navier Stokes based computational fluid dynamics for the aerodynamic assessments by coding source terms of transpiration cooling products at a heat shield surface boundary at the wind side shoulder, creating an asymmetric scheme. Study results show induced moments about the pitch axis incurred following the source terms of a cooling fluid at a near-shoulder location on the heat shield. Lift and drag saw increasing modulation with increase in mass flux rate. Pitch moment was altered a total of 388 N-m between lowest and highest 'suction' rates and changed 194 N-m maximum between 'blowing' rates.

I. Nomenclature

M	= Mach Number	σ	= Stefan-Maxwell constant, W/m^2K^4
α	= angle of attack, deg (Table 1) *and* absorptivity (eq. 1)	q	= dynamic pressure, kPa (Table 1) *and* heat flux, W/m^2
EI	= Entry Interface, s	J	= diffusive flux, kg/m^2s
x	= lateral direction		
$\dot{m}$	= mass flux, kg/m^2s	h	= specific enthalpy, J/kg
P	= pressure, Pa	Y	= species mass fraction
T	= temperature, K	ρ	= density
V	= velocity, m/s	ϵ	= emissivity
subscripts			
e	= energy flux	g	= pyrolysis gas
c	= char	i	= species index
v	= viscous	r	= radiation(incident)
w	= wall	∞	= freestream
superscripts			
-	= to solid phase	+	= from gas phase
g	= pyrolysis gas	¯	= mean value

[1] Graduate Researcher, Mechanical and Aerospace Engineering, University of Central Florida, Orlando Florida 32816 USA., Student AIAA Member

[2] Associate Professor, Mechanical and Aerospace Engineering, University of Central Florida, Orlando Florida 32816 USA., Senior AIAA Member

[3] Senior Aerospace Engineer, Structural and Thermal Systems Branch, NASA Langley Research Center, Hampton Virginia 23681 USA, AIAA Senior Member

II. Introduction

Planetary entry missions have primarily utilized single-use ablative heat shields for thermal protection through atmospheric entry. For sustained space travel, there is need for reusable entry vehicles to reduce the littering of single-use parts and promote quick mission turn-around time. This need has renewed interest in a transpiration-cooled thermal protection system that protects vehicle surfaces by means of coolant heat absorption and potentially the creation of a coolant film layer across the external boundary[1]. Improved flight trajectory controls for entry vehicles are in demand for future missions. Often, maneuvering of flight vehicles requires shape or configuration changes to perturb the vehicle attitude and ballistic characteristics on entry trajectories. The present state-of-the-art methods include reaction control system (RCS) thrusters as is relevant to the Mars Science Laboratory (Perseverance) and the currently in-development hypersonic inflatable aerodynamic decelerator that directly changes vehicle surface area and shape[2].

This work proposes to meet both mission requirements of cooling and attitude authority via a single system, tested for feasibility in numerical analysis measuring aerodynamic forces on an entry vehicle by application of source terms associated with transpiration cooling products and evaluating effective changes in thermal profiles. The surface output of local cooling conditions affects local surface pressure gradient, and in turn the vehicle moments for maneuvering on entry. The application changes the effective outer mold line (OML) and can be considered a form of porous surface control.

Porous materials are characterized by having embedded void space that can support flow through the structure. Flow through these voids is driven by pressure gradient between the external flow and internal void conditions. The overall effect of a porous feature is that it weakens pressure gradients at surfaces, or, permits a coolant to enter the void space which changes the intrinsic porosity of the material and also alters the surface pressure gradient. In supersonic flows, porous structures have been observed to affect shocks in several ways. Such effects include allowing shocked flow to enter void space, weakening compression waves near the leading edges of blunt bodies or decrease detached bow shock layer thickness. These are seen in schlieren imaging around a cylindrical leading face in supersonic flow show a decrease in shock standoff distance when replaced with a porous leading face[3]. Application of porous structures in strategic regions have been studied to take advantage of such effects. In one such numerical study, the designation of porous regions yielded results indicating the porous regions replace traditional control surfaces for effective pitch, yaw, and roll control on a conventional supersonic aircraft form[4], producing comparable control authority by enabling the porous control surface area to allow flow through.

These porous surfaces are inherent to transpiration cooled schemes. The characteristics of the cooling scheme is shown in Figure 1, giving a 2-D view of external hot gas meeting the porous medium, beneath which is the plenum of coolant fluid. The thermal gradient in the solid between a coolant reservoir and the hot external surface drives the vapor through the porous medium. The transpiration mechanism is through the coolant vapor absorbing heat from the matrix via conductive and convective heat transfer, effectively lowering the peak heat flux the external surface is exposed to in flight. Experimental studies on materials have evaluated cooling efficiency and material-specific parameters of inertial and viscous resistance of the porous matrix[5]. The primary focus of study for application of a transpiration cooling scheme is dependent on cooling efficiency and impact on boundary layer transition and stability, in interest of downstream viscous effects on heating and aerodynamic coefficients of the vehicle in whole at relevant flight conditions. To date, the authors are unaware of any study of force moment effects across an asymmetrically applied transpiration cooling scheme, as seen Figure 2. Two forms of coolant manipulation are shown: ‘blowing’ of coolant product exiting the porous surface into the external gas; and ‘suction’ at the surface by decreasing the plenum availability to transpire through the porous medium and thereby increasing its effect porosity.

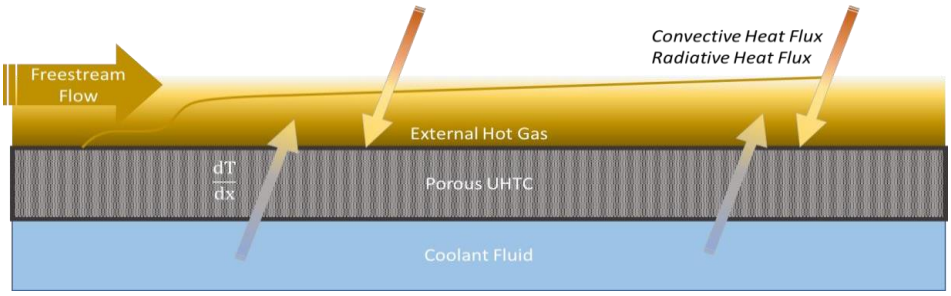

Figure 1: Diagram of the various aspects relating to a transpiration cooled surface. The upper part indicates hot air flowing over a UHTC. The coolant expands and is driven through the porous UHTC to provide cooling and alters the external flow.

Consolidating these principles warrants the study of a transpiration-cooled system on the overall pressure distribution for an entry vehicle, in addition to the limits at which the system can be manipulated to achieve trajectory-altering moments within the bounds of thermal flux.

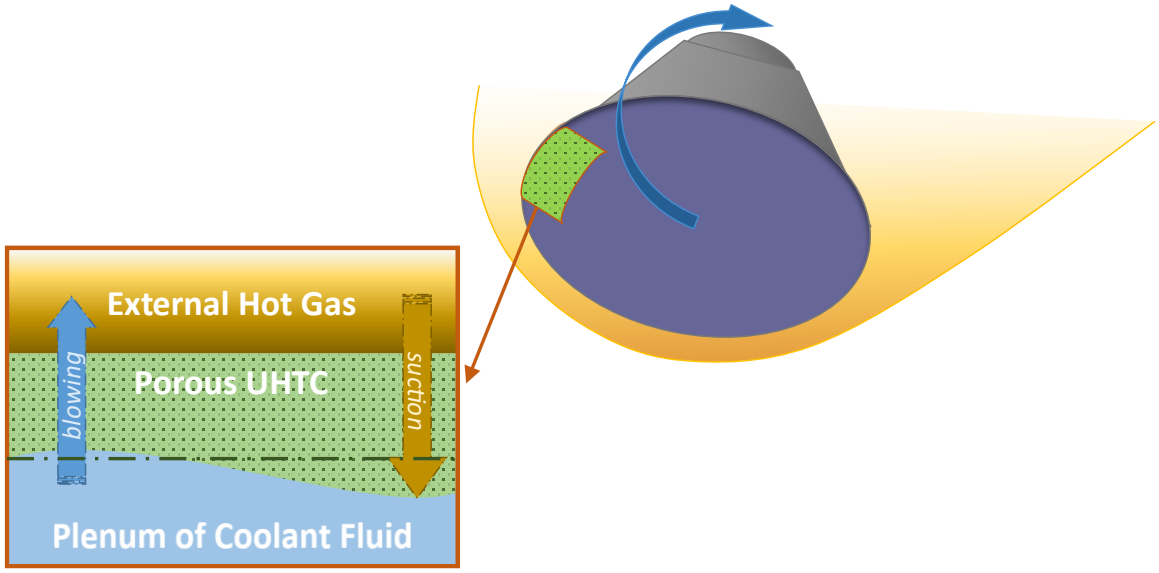

Figure 2: Illustration of local transpiration cooling effects on ballistic entry capsule heatshield inducing aerodynamic force moment

This paper will entail the numerical solutions of flow and resulting aerodynamic forces and moments from input of asymmetric application of the transpiration cooling products to evaluate aerodynamic effectiveness. A detail of methodology used in the numerical model will outline the solver, boundary conditions, and method of surface term implementation for various rates of 'blowing' and 'suction' coolant effects on the local surface. Results of measured entry capsule forces and moments are compared across rates and evaluated for effect in lift-drag modulation to use terms relevant to entry trajectory planning.

III. Methods

This numerical model builds off previous work[6]in a 3-D solution Reynolds-Averaged Navier Stokes form of conservation of mass, momentum and energy for chemical and thermal non-equilibrium flow based on Mars atmosphere composition based on an 8-species CO2-N2 model[7]. The parallel multi-block, finite-volume code Data-Parallel Line Relaxation (DPLR)[8] is a fully-implicit solver based on Gauss Siedel Line relaxation that modifies it for pointwise relaxation steps of body tangential and body normal flux vectors of the convective and viscous parts. Monotonic Upstream-centered Scheme for Conservation Laws (MUSCL) reconstruction enlists a Minmod limiter for Euler flux reconstruction, in addition to standard eigenvalue limiting in body-normal directions. Mixture viscosity and thermal conductivity follow Yos approximate mixing rules.

The model solves implicitly for steady-state solution based on freestream conditions listed in Table 1, with reference to the atmospheric recreation of trajectory followed by Mars Science Laboratory entry vehicle[9].

Table 1: Simulation Freestream Conditions with reference to Martian Entry Capsule at 130s Into Entry Interface [9]

EI Time (s)	Altitude (km)	V_∞ (m/s)	T_∞ (K)	ρ_∞ (kg/m^3)	M_∞	α (deg)	$\bar{q}$ (kPa)
130	14.3	1263.5	192.2	4.396E-03	5.7	-18.58	3.51

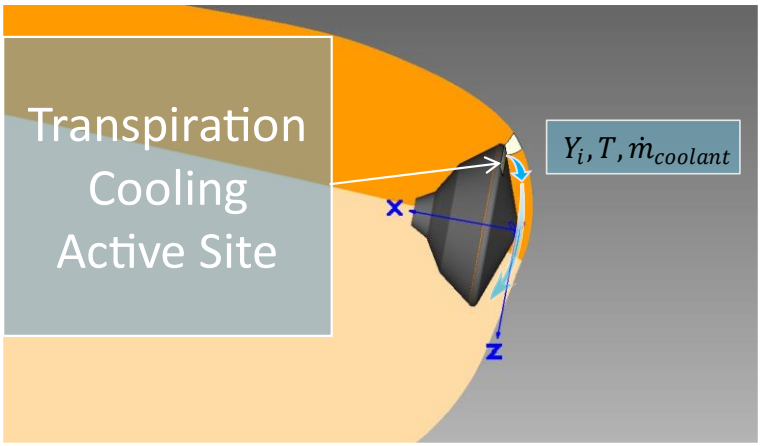

Figure 3: 3D domain split down pitch plane for entry capsule at angled entry highlighting part of domain where source terms are injected at the capsule surface boundary

At a selected surface near the capsule shoulder on wind side, highlighted in Figure 3, source terms of species mass fraction, temperature and mass flux rate are defined. Two forms of transpiration cooling scheme manipulation are implemented: positive mass flux into the flow domain to simulate an excess of transpiration cooling product entering the flow in a 'blowing' manner compared with the rest of the heatshield's passively cooled state; and negative mass flux out of the domain in a manner similar to the 'suction' of porous surface control methods described in II. The source term method including definition of temperature, however, is not true to application of the 'suction' variant, and instead used purely for aerodynamic evaluation.

The source terms are implemented via Dirichlet type boundary developed in effort[10] for coupling to material response solver, where solution of the CFD allows input of surface heat flux to the material response solver. This is the boundary on which mass fractions and overall mass flux rate are defined to the CFD surface boundary. Energy balance across this boundary follows eq. 1, in conjunction with eq. 2, where the boundary layer edge solves in the absence of a char product.

$$q_c^- = q_c^+ + \sum_i h_i J_i + q_v^+ - \dot{m}_g \sum_i h_i (Y_i - Y_i^g) - \dot{m}_c (\sum_i h_i Y_i - h_c) + \alpha q_r - \epsilon \sigma T_w^4 \quad (1)$$

$$q_e^+ = q_c^+ + q_v^+ + \sum_i h_i J_i$$

2

The rest of the capsule surface is defined as a non-slip, radiative equilibrium wall with assumption of super catalytic handling of wall species returning to freestream values. A constant emissivity is assumed of 85% to solve standard Stefan-Boltzmann equation of heat balance with respect to the viscous and diffusive contributions at wall. This process is designed for goal of coupling with material response solver to accurately represent transpiration cooling output and iteratively determine coupled effects of external material and coolant responses.

The purpose of this 'activated' surface is to explore the application of asymmetric cooling input for the goal of capsule attitude adjustments. It is assumed this will closely resemble in aerodynamic coefficient terms a realistic cooling scenario across the entire heatshield, in which selected shoulder regions are manipulated for desired change in force moment result. Methods of importance in this model's convergence include pulling solutions through ramped increase of mass injection rates, by altering source term mass flux value in a series process. A laminar solution is developed prior to applying a turbulence closure model, which is desired for the viscous effects at and downstream of the perturbance region.

Convergence is monitored across several heatshield surface points of heat flux values for 6-order of magnitudes decrease. These points were selected across the selected surface region of perturbance, and for comparison, points within the stagnation zone. Also monitored was global residual of momentum and energy equations. Finally, measured aerodynamic forces and moments based on the Mars Science Laboratory mass properties[11][12] for minimum 4 magnitudes of decrease.

IV. Results

Results from this study focus foremost on the changes aerodynamic forces and moments measured about the entry capsule as result of the asymmetric cooling scheme applied. Directional force sums and total moments are plotted across the tested mass flux rates. Mass flux rates were applied in two forms: positive, indicating a blowing of coolant into the boundary layer of the vehicle, and suction, indicating a withdrawal of coolant through the external porous surface akin to the porous surface control examples in II. Capsule coordinate system forces (top row) and force moments (bottom row) are shown in Figure 4. The initiation of mass flux terms creates a swift change in forces and resulting moments that shows and increasing trend in change as mass flux rate increases, rounding out towards a plateau in mass flux rates of 0.06 kg/m^2s and 0.1 kg/m^2s. Suction cases showed less force impact than blowing cases but makes a larger difference in axial and normal plane forces towards the highest mass flux rate of 0.6 kg/m^2s. This makes a marked difference in pitch moment, M_y between the two methods.

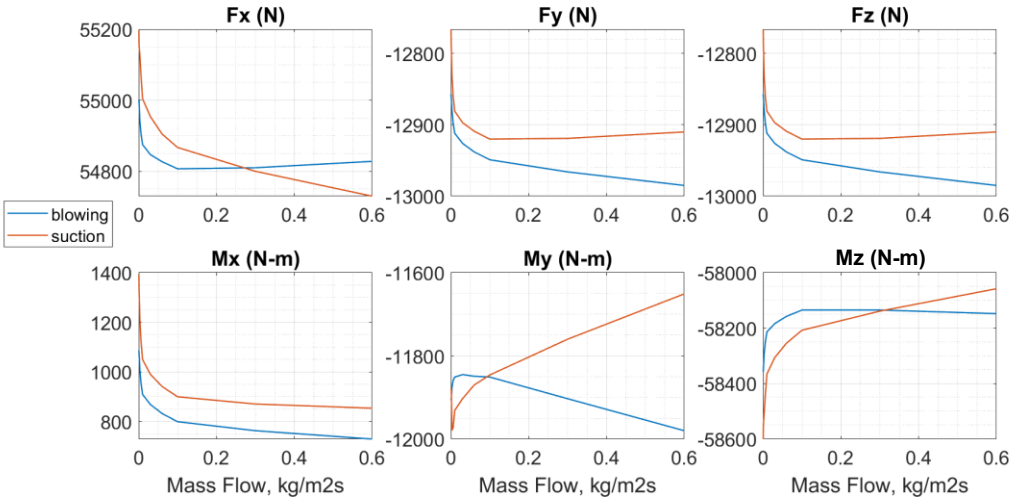

Figure 4: Capsule coordinate system forces and moments across mass fluxes for blowing and suction

The results are translated to vectors of vehicle lift and drag[13]. The edited diagram in Figure 5 shows the lift and drag directions of the capsule in the frame of the wind coordinate system for reference. This measurement is used to provide a sense of overall aerodynamic impact from the asymmetric scheme across the heatshield.

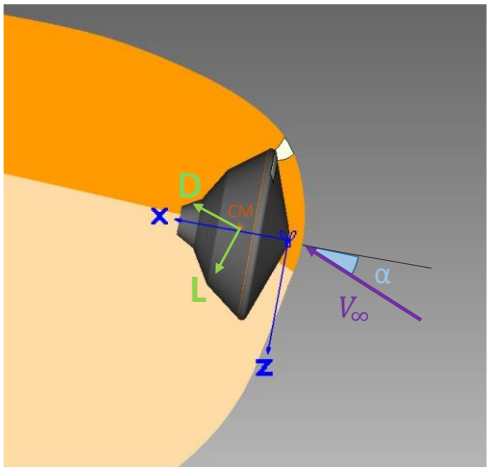

Figure 5: Lift and Drag directions for wind coordinate system designated on the capsule CG

The values of lift are plotted in Figure 6, where it is seen that applying an increase of mass flux of either blowing or suction at the wind-side shoulder has increased lift values for the vehicle. The rate of increase starts to decline with increasing mass flux, and suction seems to approach the effect on lift that blowing takes in the higher mass flux rates. This result is counter to expected results, which intuitively would show decreasing lift values for the suction cases. This implies a need for further investigation to surface pressure at region of surface source terms applied. In conjunction, the source term application method included prescribing a constant surface temperature assumed to be constant with near reservoir coolant temperature, of 300 K. The surface pressure is solved in this method by assuming thermal equilibrium at the surface, thus yielding a similar profile to the blowing application.

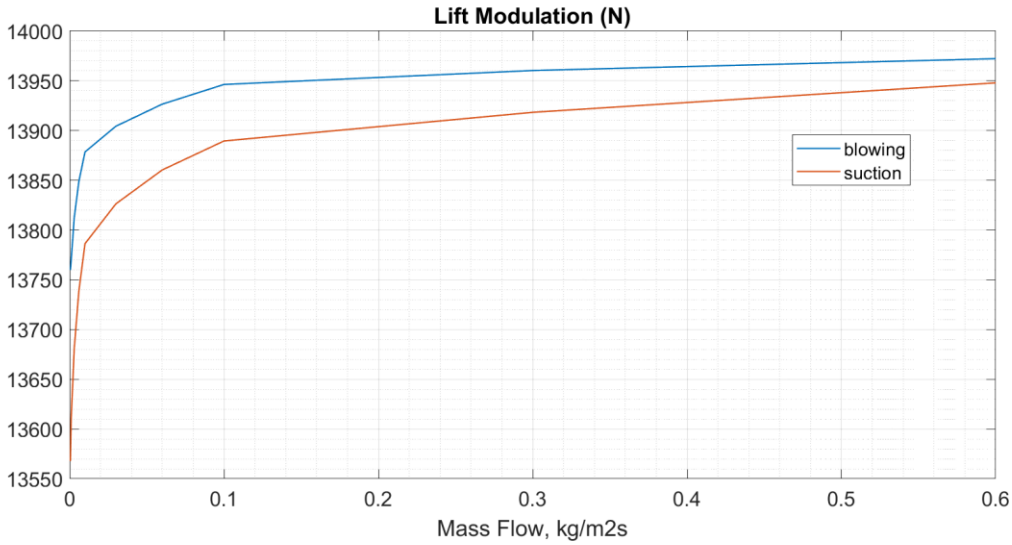

Figure 6: Lift modulation across mass flux rates

Adjusting the boundary condition for suction cases will be crucial to extracting surface pressure as a function of mass flux rate for input to a material response solver as related to iteratively ensuring transpiration cooling is accurately represented.

The drag force modulation is plotted in Figure 7, showing a significant decrease at lowest mass flux rate of 0.6 kg/m^2s that exceeds that of the blowing case.

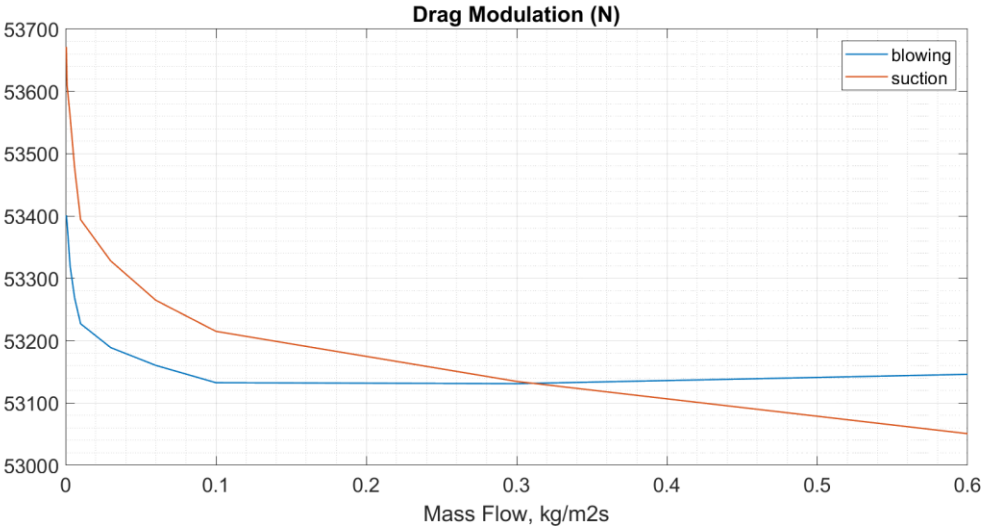

Figure 7: Drag modulation across mass flux rates

Finally, lift-drag ratio is plotted in Figure 8, where a changes of magnitude 10^{-3} are seen between mass flux rates. Quantification of control authority is referred to 9.4.1.3 of the 2015 NASA Technology Roadmaps[14]which designated lift-drag ratio between 0.15 to 0.20 and a change in rate of 0.005 – 0.008.

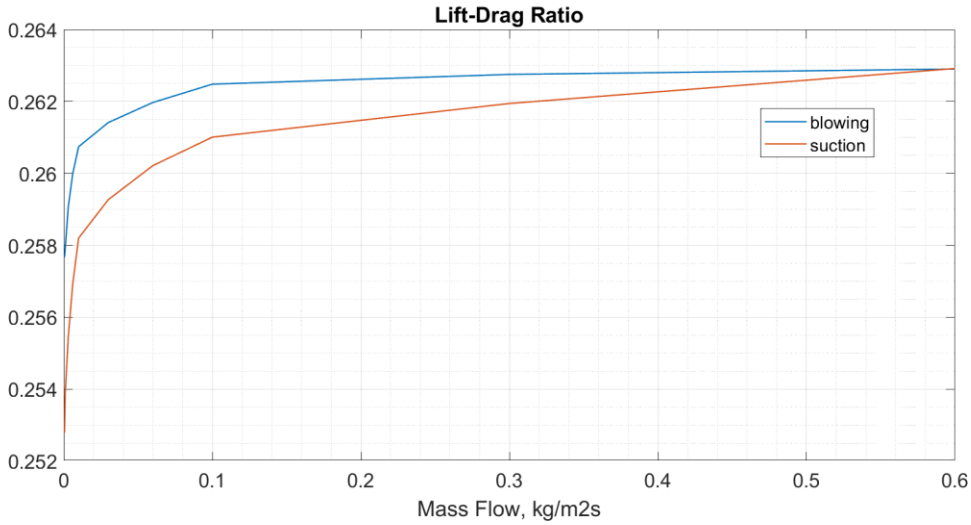

Figure 8: Lift-Drag ratio for blowing and suction applications across increasing mass flux rates of an asymmetric cooling scheme

The model desires a turbulence closure model, not only to address the behavior of source term effects but to also replicate reference flight conditions to greater accuracy, given the Mars Science Laboratory entry capsule saw transition along the heatshield well before this time point along the entry interface. In Figure 9, the Baldwin-Lomax model is applied to an earlier study of the laminar blowing results with isothermal non-blowing wall conditions for observation. The turbulent solution increases forces read for blowing solutions across the axial and normal directions on the vehicle, resulting in a higher pronounced pitch moment. The difference between the models seem to diminish with increasing mass blowing rate.

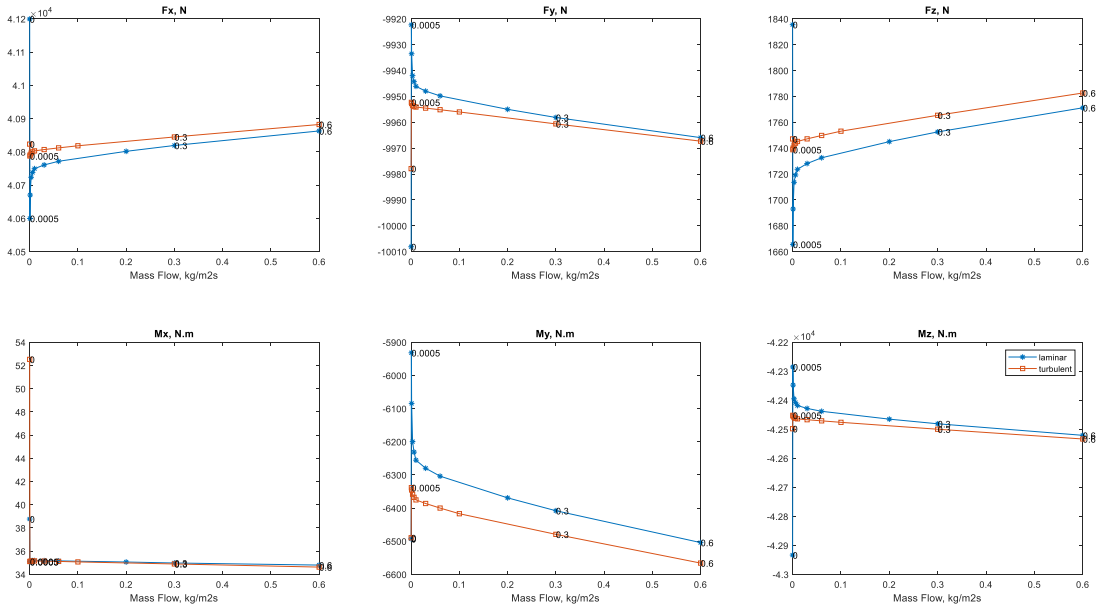

Figure 9: force and moment comparison for blowing cases under laminar and turbulent conditions

V. Conclusions

A numerical model of a Martian entry capsule is numerically resolved in a steady state solution of Reynolds-Averaged Navier Stokes at low hypersonic flight conditions. By utilizing a boundary condition attuned for source term implementation based on material solver coupling, an asymmetric scheme of cooling products are applied on the heatshield wind side shoulder to simulate two forms: 'blowing' of excess coolant and 'suction' of available transpiration coolant. Based on the results the injected coolant had a minimal effect on the bulk flow but show load control of 10^{-3} on pitch moment between mass flux rates tested. The magnitude is observed in the study is on par with magnitude of lift-drag ratio acceleration goals per Technology Roadmaps of 2015 goals. The suction cases exhibited similar behavior to that of the blowing, due to the used constant temperature boundary's solution of extrapolated pressure given thermal equilibrium, albeit less lift-drag ratio modulation than blowing conditions shown. Suction, however, seems to show ongoing drag modulation beyond blowing condition's effective impact with increasing mass flux rate.

The model is continuing development to include turbulent responses to compare with laminar solutions. Preliminary results with blowing conditions show an increase in radial and normal force magnitudes. This comparison also hopes to lend insight to transition potential due to source term implementation upstream on the heatshield. Source term implementation is also under development with parallel development of material response solver for truer transpiration cooling conditions, and surface temperature definition at the surface boundary(ies).

Acknowledgments

This work is sponsored via 2021 NSTGRO Fellowship through the. National Aeronautics and Space Administration under Grant/Contract/Agreement No. 80NSSC21K1256 P00002. Many thanks to Jeffrey Hill and Dinesh Prabhu at NASA Ames Research Center for assistance in troubleshooting code.

References

[1] Glass, D. E., Dilley, A. D., and Kelly, H. N., "Numerical Analysis of Convection/Transpiration Cooling," *Journal of Spacecraft and Rockets*, Vol. 38, No. 1, 2001, pp. 15–20. https://doi.org/10.2514/2.3666

[2] Green, J. S., Goyne, C., and Mcdaniel, J., "Morphing Hypersonic Inflatable Aerodynamic Decelerator," 2012.

[3] Maslov, A. A., Mironov, S. G., Poplavskaya, T. V., and Kirilovskiy, S. V., "Supersonic Flow around a Cylinder with a Permeable High-Porosity Insert: Experiment and Numerical Simulation," *Journal of Fluid Mechanics*, Vol. 867, 2019, pp. 611–632. https://doi.org/10.1017/jfm.2019.165

[4] Hunter, C. A., Viken, S. A., Wood, R. M., and Bauer, S. X. S., "Advanced Aerodynamic Design of Passive Porosity Control Effectors," *39th Aerospace Sciences Meeting and Exhibit*, No. August, 2001. https://doi.org/10.2514/6.2001-249

[5] Hermann, T., Naved, I., and McGilvray, M., "Performance of Transpiration Cooled Heat Shields for Re-Entry Vehicles," *AIAA Scitech 2019 Forum*, No. January, 2019. https://doi.org/10.2514/6.2019-1778

[6] Anderson, C., and Kinzel, M. P., "Numerical Evaluation of Entry System Trajectory Control via Active Porosity Control of Transpiration Cooled Thermal Protection System," No. January, 2023, pp. 1–11. https://doi.org/10.2514/6.2023-0391

[7] Mitcheltree, R. A., and Gnoffo, R. A., "Wake Flow about the Mars Pathfinder Entry Vehicle," *Journal of Spacecraft and Rockets*, Vol. 32, No. 5, 1995, pp. 771–776. https://doi.org/10.2514/3.26682

[8] Wright, M. J., Candler, G. V., and Bose, D., "Data-Parallel Line Relaxation Method for the Navier-Stokes Equations," *AIAA Journal*, Vol. 36, No. 9, 1998, pp. 1603–1609. https://doi.org/10.2514/2.586

[9] Edquist, K. T., Hollis, B. R., Johnston, C. O., Bose, D., White, T. R., and Mahzari, M., "Mars Science Laboratory Heat Shield Aerothermodynamics: Design and Reconstruction," *Journal of Spacecraft and Rockets*, Vol. 51, No. 4, 2014, pp. 1106–1124. https://doi.org/10.2514/1.A32749

[10] Cruden, B. A., "On the Fluid Dynamics Boundary Condition in Ablating or Blowing Flows," No. June, 2023, pp. 1–18. https://doi.org/10.2514/6.2023-3614

[11] Karlgaard, C. D., Kutty, P., Schoenenberger, M., Munk, M. M., Little, A., Kuhl, C. A., and Shidner, J., "Mars Science Laboratory Entry Atmospheric Data System Trajectory and Atmosphere Reconstruction," *Journal of Spacecraft and Rockets*, Vol. 51, No. 4, 2014, pp. 1029–1047. https://doi.org/10.2514/1.A32770

[12] Dyakonov, A. A., Schoenenberger, M., and Van Norman, J. W., "Hypersonic and Supersonic Static Aerodynamics of Mars Science Laboratory Entry Vehicle," 2012. https://doi.org/10.2514/6.2012-2999

[13] Schoenenberger, M., Van Norman, J., Karlgaard, C., Kutty, P., and Way, D., "Assessment of the Reconstructed Aerodynamics of the Mars Science Laboratory Entry Vehicle," Vol. 51, 2014, pp. 1076–1093. https://doi.org/10.2514/1.A32794

[14] NASA, "NASA Technology Roadmaps," 2015.